Optics
2013; 2(1) : 7-16
Published online February 20, 2013 (http://www.sciencepublishinggroup.com/j/optics)
doi: 10.11648/j. optics.20130201.12

Nonlinear amplification of the brillouin-rayleigh triplet caused by two-photon heating

V. B. Karpov*, V. V. Korobkin

Coherent and Nonlinear Optics Department, A.M.Prokhorov General Physics Institute, Russian Academy of Sciences, Vavilov Street 38, 119991 Moscow, Russia

Email address:
karpov@kapella.gpi.ru (V. B. Karpov)

To cite this article:
V. B. Karpov, V. V. Korobkin. Nonlinear Amplification of the Brillouin-Rayleigh Triplet Caused by Two-Photon Heating, *Optics.* Vol. 2, No. 1, 2013, pp. 7-16. doi: 10.11648/j.optics.20130201.12

Abstract: The thin structures of stimulated Brillouin scattering (SBS) and stimulated temperature scattering (STS) spectral components caused by two-photon heating are analyzed theoretically. In contrast to the linear (single-photon) case for two-photon heating a stokes SBS component exhibits the spectral shift depending on the pump intensity. Emergence of an anti-stokes SBS component is possible when the pump intensity is sufficiently high so that the positive two-photon thermal gain may compensate the negative electrostrictive gain. The spectral components of STS caused by linear or two-photon absorption (essentially different linear or two-photon STS-2) possess the same thin structures.

Keywords: Nonlinear Optics; Stimulated Brillouin Scattering (SBS); Stimulated Temperature Scattering (STS); Brillouin-Rayleigh Triplet; Two-Photon Heating; Stokes and Anti-Stokes Components; Near Ultraviolet Radiation; Excimer Lasers

1. Introduction

For high enough light intensity and coherence the well-known weak spontaneous Brillouin-Rayleigh triplet [1, 2] transforms into the powerful doublet of a “slightly” anti-stokes shifted line of stimulated temperature scattering (STS) caused by linear (single-photon) or two-photon absorption (linear or two-photon STS-2) and a “strongly” stokes shifted line of stimulated Brillouin scattering (SBS). Various experiments display the doublet’s lines singly or grouped. For the near-ir spectral region (the pump wavelength is $\lambda_1 = 0.69 \div 1.06\,\mu m$) such a transformation has been originally observed in [3, 4]. For the near-uv spectral region ($\lambda_1 = 193 \div 351 nm$) such a transformation has been originally observed in [5, Fig. 2]. Indeed, in the previous near-uv studies [6 - 14] two-photon STS-2 lines have been associated mistakenly with SBS and linear STS-2 lines [5].

SBS is the unique high-efficiency converter of a coherent light wave (hereinafter called the pump wave that carries the pump intensity I_P) into a coherent hyperacoustical wave. Also SBS is the nonlinear-optical phenomenon providing phase conjugation (PC) of the best quality [15, 16], [5, Fig. 3]. There are two physical mechanisms responsible for nonlinear amplification of the scattered and hyperacoustical waves during an SBS process [1, 2, 4, 17, 18]. The first one (hereinafter called the conventional SBS) is due to a local variation of pressure caused by the electrostrictive force [19 - 22]. The second one (hereinafter called the thermal SBS) is attributed to a local variation of pressure caused by the thermal expansion. For the linear light absorption the thermal SBS (hereinafter called the linear thermal SBS) has been discussed in [23 - 25].

The purely conventional SBS was considered in [5], the thermal SBS was ignored. This is a quite typical approximation, used for instance in the study of the PC provided by SBS [15], when information gained from roughly measured spectral shifts is enough. It should be noted that too rough measurements can lead to a loss of new physics. Such a loss of the genuine SBS for the near-uv, the two-photon STS-2, and other effects [5] has happened in [6 - 14].

Following [5], the unshifted lines in the left sides of [5, Fig. 2] (relative to the pump ones in the right sides) correspond to the linear and two-photon STS-2; the shifted lines correspond to the genuine conventional SBS. The observation of the thin structures of these lines including the pump ones is restricted by a Fabry-Perot etalon based spectrum analyzer [5]. The spectral resolution of a Fabry-Perot etalon is limited by several MHz (or $10^{-3}\ cm^{-1}$) [26]. To reach the higher spectral resolution methods of

heterodyning and intensity fluctuations correlation should be used. An experimental high-resolution spectral profile of a Brillouin line exhibiting an antisymmetrical behavior is given in [27].

In this paper, a contribution of the two-photon heating to the thermal SBS (hereinafter called the two-photon thermal SBS) modifying the stokes and anti-stokes branches is considered. The thin structure of a two-photon STS-2 line first experimentally discovered in [5] was not studied theoretically and is also a subject of interest.

An effective linear absorption coefficient $\alpha_{eff}(\omega)$ has been introduced [24] for gases to describe the thermalization processes of the absorbed electromagnetic energy. In our analysis a total absorption coefficient [5]

$$\alpha_\Sigma = \alpha + (I_P \gamma), \qquad (1)$$

should be used to describe the two-photon effect (α is a linear absorption coefficient and γ is a two-photon absorption coefficient).

2. Mass (Bulk) and Serface Forces

The theory of the coupling of light and elastic waves is based on the Lagrange equation [19, 20]. In [19] a nonlinear system was developed and a linearized system for small perturbations has been solved. The photoelastic coupling of a longitudinal acoustic wave in an isotropic medium was studied in [20], and the nonlinear system from [19] including the saturation effect has been solved.

The Lagrange equation [28] describes the mechanics of discrete bodies. It takes into account the mass (bulk) forces and ignores the surface ones. For continuous media both mass and surface forces should be incorporated [29, 30] and the Navier-Stokes equation is used instead of the Lagrange one. Indeed, any plane acoustic wave propagating in a continuous medium provides shear motion leading to the attenuation due to viscosity η [31] (see (2) below).

3. Material Equations

Interaction of a light wave, characterized by a total electrical field vector $\boldsymbol{E}$, with an isotropic dielectric medium is described by the hydrodynamic equations linearized with respect to the small deviations of density $\Delta\rho$, temperature ΔT, pressure ΔP, and a macroscopic velocity vector $\boldsymbol{V}$ from the equilibrium values ρ_0, T_0, P_0, and $\boldsymbol{V}_0 = 0$ [1, 2, 4, 17, 32]:

$$\rho_0 \frac{\partial \mathrm{V}}{\partial \mathrm{t}} + \frac{\mathrm{v}^2}{\delta}\mathrm{grad}(\Delta\rho) + \frac{\mathrm{v}^2\beta\rho_0}{\delta}\mathrm{grad}(\Delta\mathrm{T}) - \eta\nabla^2\mathrm{V} = \frac{\gamma^e}{8\pi}\mathrm{grad}(\mathrm{E}^2), \qquad (2)$$

$$\frac{\partial}{\partial t}(\Delta\rho) + \rho_0 div(\boldsymbol{V}) = 0, \qquad (3)$$

$$\left(\rho_0 c_V \frac{\partial}{\partial t} - \lambda_T \nabla^2\right)(\Delta T) - \frac{c_V(\delta-1)}{\beta}\frac{\partial}{\partial t}(\Delta\rho) = \frac{nc\alpha_\Sigma}{4\pi}(\boldsymbol{E}^2) - \frac{1}{8\pi}\left(\frac{\partial\varepsilon}{\partial T}\right)_p\left(T_0\frac{\partial}{\partial t}(\boldsymbol{E}^2)\right). \qquad (4)$$

Here $v = \sqrt{\frac{1}{\rho_0\beta_S}}$ is the speed of sound in a medium with adiabatic compressibility β_S, c is the speed of light in vacuum, $\delta = \frac{c_P}{c_V}$ is a ratio of specific heats (a frequently used symbol γ in (1) provides the logical connection with [5]), $\beta = -\frac{1}{\rho_0}\left(\frac{\partial\rho}{\partial T}\right)_P$ is a volumetric thermal expansion coefficient at constant pressure, $\gamma^e = \rho_0\left(\frac{\partial\varepsilon}{\partial\rho}\right)_T$ is an electrostriction coefficient, λ_T is thermal conductivity, and n is a refractive index.

In the Navier-Stokes equation (2) the pressure deviation is expressed as [23, 24, 33 - 35]:

$$\Delta P = \frac{v^2}{\delta}(\Delta\rho) + \frac{v^2}{\delta}\rho_0\beta(\Delta T),$$

and its gradient is moved into the left-hand side ($grad\, P_0 = 0$). The right-hand side of (2) represents the electrostrictive force [35]. The first and second right-hand side terms of the heat equation (4) represent heating due to the light absorption (both the linear and two-photon introduced by α_Σ) and heating due to the electrocaloric effect [1, 36], respectively.

The Navier-Stokes equation (2) and the continuity equation (3) can be combined into one by eliminating the macroscopic velocity vector $\boldsymbol{V}$:

$$\left(-\frac{\partial^2}{\partial t^2} + \frac{v^2}{\delta}\nabla^2 + \frac{\eta}{\rho_0}\frac{\partial}{\partial t}\nabla^2\right)(\Delta\rho) + \frac{v^2\beta\rho_0}{\delta}\nabla^2(\Delta T) = \frac{\gamma^e}{8\pi}\nabla^2(E^2). \qquad (5)$$

An ideal dielectric medium with uniform optical properties cannot scatter light. Both spontaneous (SP) and stimulated (NL) manners of the scattering arise from permittivity variation about the equilibrium value ε_0:

$$\Delta\varepsilon = \Delta^{SP}\varepsilon + \Delta^{NL}\varepsilon = \left(\frac{\partial\varepsilon}{\partial\rho}\right)_T\Delta\rho + \left(\frac{\partial\varepsilon}{\partial T}\right)_\rho\Delta T = \left(\frac{\partial\varepsilon}{\partial\rho}\right)_T(\Delta^{SP}\rho + \Delta^{NL}\rho) + \left(\frac{\partial\varepsilon}{\partial T}\right)_\rho(\Delta^{SP}T + \Delta^{NL}T).$$

Usually [1, 2, 17, 32]

$$\left|\left(\frac{\partial\varepsilon}{\partial\rho}\right)_T \Delta^{NL}\rho\right| >> \left|\left(\frac{\partial\varepsilon}{\partial T}\right)_\rho \Delta^{NL}T\right|,$$

$$\left(\frac{\partial\varepsilon}{\partial T}\right)_P \approx -\beta\left(\rho_0\frac{\partial\varepsilon}{\partial\rho}\right)_T . \quad (6)$$

The task has been provided by the material equations (4) and (5) involving independent variables $\Delta\rho$ and ΔT, and as a new element a total absorption coefficient α_Σ.

4. SBS and STS Gain

Physically speaking SBS and STS are nonresonant parametric phenomena [22, 37]. (Simulated Raman scattering is a resonant parametric phenomenon.)

Consider two counterpropagating linearly polarized plane electromagnetic waves, a pump wave and a backscattered wave, characterized by electrical field vectors $\boldsymbol{E}_P$ and $\boldsymbol{E}_S$:

$$\boldsymbol{E}_P = \frac{1}{2}\boldsymbol{e}\left\{E_1(z,t)\exp(ik_1z - i\omega_1t) + c.c.\right\}, \quad (7)$$

$$\boldsymbol{E}_S = \frac{1}{2}\boldsymbol{e}\left\{E_2(z,t)\exp(-ik_2z - i\omega_2t) + c.c.\right\}. \quad (8)$$

Here, $\boldsymbol{e}$ is a common [21] unit vector (for definiteness sake $\boldsymbol{e} = \boldsymbol{e}_X$); $E_1(z,t)$ and $E_2(z,t)$ are complex amplitudes; ω_1, ω_2 and k_1, k_2 are temporal frequencies and wave numbers, respectively. A total electric field vector is

$$\boldsymbol{E} = \boldsymbol{E}_P + \boldsymbol{E}_S . \quad (9)$$

The linear (L) and nonlinear (NL) electrical induction vectors are [21, 22, 37]

$$\boldsymbol{D}^L(z,t) = \hat{\varepsilon}(\omega)\boldsymbol{E}(z,t),$$

$$\boldsymbol{D}^{NL}(z,t) = \hat{\varepsilon}^{NL}(\omega,z,t)\boldsymbol{E}(z,t),$$

where $\hat{\varepsilon}(\omega)$ and $\hat{\varepsilon}^{NL}(\omega,z,t)$ are the Fourier transforms of the linear and nonlinear permittivity tensors $\hat{\varepsilon}(t_1)$ and $\hat{\varepsilon}^{NL}(t_1,t_2,t_3)$ [22, 37]. For the isotropic medium the tensors are replaced by the scalars [22, 37]:

$$\boldsymbol{D}^L(z,t) = \varepsilon(\omega)\boldsymbol{E}(z,t),$$

$$\boldsymbol{D}^{NL}(z,t) = \varepsilon^{NL}(\omega,z,t)\boldsymbol{E}(z,t) \cong$$

$$\cong \left(\left(\frac{\partial\varepsilon}{\partial\rho}\right)_T \Delta^{NL}\rho(z,t) + \left(\frac{\partial\varepsilon}{\partial T}\right)_\rho \Delta^{NL}T(z,t)\right)\boldsymbol{E}(z,t) \cong$$

$$\cong \left(\frac{\partial\varepsilon}{\partial\rho}\right)_T \Delta^{NL}\rho(z,t)\boldsymbol{E}(z,t) .$$

Accordingly, the linear and nonlinear polarization vectors are [21]

$$\boldsymbol{P}^L(z,t) = \frac{\varepsilon(\omega)-1}{4\pi}\boldsymbol{E}(z,t),$$

$$\begin{aligned} \mathrm{P}^{\mathrm{NL}}(\mathrm{z},\mathrm{t}) &= \frac{1}{4\pi}\varepsilon^{\mathrm{NL}}(\omega,\mathrm{z},\mathrm{t})\mathrm{E}(\mathrm{z},\mathrm{t}) \\ &\cong \frac{1}{4\pi}\left(\frac{\partial\varepsilon}{\partial\rho}\right)_{\mathrm{T}} \Delta^{\mathrm{NL}}\rho(\mathrm{z},\mathrm{t})\mathrm{E}(\mathrm{z},\mathrm{t}) \end{aligned} . \quad (10)$$

The waves are coupled by the scalar electrodynamical equations [1, 2, 17, 32, 37]

$$\left[\nabla^2 - \frac{\varepsilon(\omega_1)}{c^2}\frac{\partial^2}{\partial t^2}\right]\boldsymbol{E}_P = \frac{4\pi}{c^2}\frac{\partial^2}{\partial t^2}\boldsymbol{P}^{NL}_{\omega_1}, \quad (11)$$

$$\left[\nabla^2 - \frac{\varepsilon(\omega_2)}{c^2}\frac{\partial^2}{\partial t^2}\right]\boldsymbol{E}_S = \frac{4\pi}{c^2}\frac{\partial^2}{\partial t^2}\boldsymbol{P}^{NL}_{\omega_2}, \quad (12)$$

with the right-hand sides representing the nonlinear polarizations oscillating with the frequencies ω_1 and ω_2. For the plane waves diffraction is absent ($\left[\frac{\partial^2}{\partial x^2}+\frac{\partial^2}{\partial y^2}\right]\boldsymbol{E}_{P,S}(z,t)=0$).

Following (4) and (5) the nonlinearity of (10) is due to the dependence of $\Delta\rho \cong \Delta^{NL}\rho$ and $\Delta T \cong \Delta^{NL}T$ on the scalar product $\boldsymbol{E}^2$. We seek the steady-state solution (the complex amplitudes do not depend on t) based on the slowly oscillating part of $\boldsymbol{E}^2$

$$\begin{aligned} \left\langle \mathrm{E}^2\right\rangle &= \left\langle(\mathrm{E_P}+\mathrm{E_S})^2\right\rangle = \left\langle 2\mathrm{E_P}\mathrm{E_S}\right\rangle = \\ &= \frac{1}{2}\left\{\mathrm{E}_1(\mathrm{z})\mathrm{E}_2^*(\mathrm{z})\exp\begin{bmatrix}-\mathrm{i}(\omega_1-\omega_2)\,\mathrm{t}\\ +\mathrm{i}(\mathrm{k}_1+\mathrm{k}_2)\,\mathrm{z}\end{bmatrix} + \mathrm{c.c.}\right\}, \end{aligned} \quad (13)$$

and the appropriate approximations for $\Delta^{NL}\rho$ and $\Delta^{NL}T$

$$\Delta^{\mathrm{NL}}\rho(\mathrm{z},\mathrm{t}) = \frac{1}{2}\left\{\rho_{\mathrm{a}}(\mathrm{z})\exp\begin{bmatrix}-\mathrm{i}(\omega_1-\omega_2)\,\mathrm{t}\\ +\mathrm{i}(\mathrm{k}_1+\mathrm{k}_2)\,\mathrm{z}\end{bmatrix} + \mathrm{c.c.}\right\}, \quad (14)$$

$$\Delta^{\mathrm{NL}}\mathrm{T}(\mathrm{z},\mathrm{t}) = \frac{1}{2}\left\{\mathrm{T}_{\mathrm{a}}(\mathrm{z})\exp\begin{bmatrix}-\mathrm{i}(\omega_1-\omega_2)\,\mathrm{t}\\ +\mathrm{i}(\mathrm{k}_1+\mathrm{k}_2)\,\mathrm{z}\end{bmatrix} + \mathrm{c.c.}\right\}. \quad (15)$$

On substitution of (6), (13) - (15) into (4) and (5), a linear system for the complex amplitudes $\rho_a(z)$, $T_a(z)$ and for the product $E_1(z)E_2^*(z)$ is found

$$\begin{aligned}&\left(-\Omega^2+\frac{v^2}{\delta}q^2+i\frac{\eta}{\rho_0}q^2\Omega\right)\rho_a\\&+\frac{v^2\beta\rho_0}{\delta}q^2T_a=\frac{1}{8\pi}\left(\rho_0\frac{\partial\varepsilon}{\partial\rho}\right)_T q^2E_1E_2^*\end{aligned}\tag{16}$$

$$\begin{aligned}&i\Omega\frac{c_V(\delta-1)}{\beta}\rho_a+\left(-i\rho_0c_V\Omega+\lambda_Tq^2\right)T_a=\\&=\frac{1}{4\pi}nc\alpha_\Sigma E_1E_2^*-\frac{i}{8\pi}\left(\rho_0\frac{\partial\varepsilon}{\partial\rho}\right)_T\beta T_0\Omega E_1E_2^*\ ,\end{aligned}\tag{17}$$

where $q=k_1+k_2$, $\Omega=\omega_1-\omega_2$. Solving (16) for T_a

$$T_a=\frac{\delta}{q^2v^2\beta\rho_0}\left[\begin{array}{l}\frac{1}{8\pi}\left(\rho_0\frac{\partial\varepsilon}{\partial\rho}\right)_T q^2E_1E_2^*-\\\left(-\Omega^2+\frac{v^2}{\delta}q^2+i\frac{\eta}{\rho_0}q^2\Omega\right)\rho_a\end{array}\right]$$

and inserting the result into (17) we obtain

$$\begin{aligned}&i\Omega\frac{c_V(\delta-1)}{\beta}\rho_a\\&+\frac{\delta\left(-i\rho_0c_V\Omega+\lambda_Tq^2\right)}{q^2v^2\beta\rho_0}\left[\begin{array}{l}\frac{1}{8\pi}\left(\rho_0\frac{\partial\varepsilon}{\partial\rho}\right)_T q^2E_1E_2^*\\-\left(\begin{array}{l}-\Omega^2+\frac{v^2}{\delta}q^2\\+i\frac{\eta}{\rho_0}q^2\Omega\end{array}\right)\rho_a\end{array}\right]=\\&=\frac{1}{4\pi}\left[nc\alpha_\Sigma-\frac{i}{2}\left(\rho_0\frac{\partial\varepsilon}{\partial\rho}\right)_T\beta T_0\Omega\right]E_1E_2^*.\end{aligned}$$

Rearrangement of ρ_a and $E_1E_2^*$ into the opposite sides gives

$$\begin{aligned}&\rho_a\left[\begin{array}{l}i\Omega\frac{c_V(\delta-1)}{\beta}-\\\frac{\delta\left(-i\rho_0c_V\Omega+\lambda_Tq^2\right)}{q^2v^2\beta\rho_0}\left(\begin{array}{l}-\Omega^2+\frac{v^2}{\delta}q^2\\+i\frac{\eta}{\rho_0}q^2\Omega\end{array}\right)\end{array}\right]=\\&=E_1E_2^*\left[\begin{array}{l}\frac{\delta\left(i\rho_0c_V\Omega-\lambda_Tq^2\right)}{8\pi q^2v^2\beta\rho_0}\left(\rho_0\frac{\partial\varepsilon}{\partial\rho}\right)_T q^2\\+\frac{1}{4\pi}\left[nc\alpha_\Sigma-\frac{i}{2}\left(\rho_0\frac{\partial\varepsilon}{\partial\rho}\right)_T\beta T_0\Omega\right]\end{array}\right].\end{aligned}$$

Upon multiplying the both sides by $\left(-\frac{8\pi q^2v^2\beta\rho_0}{\delta}\right)$ we have

$$\begin{aligned}&8\pi\rho_a\left[\begin{array}{l}\left(\begin{array}{l}-\Omega^2+\frac{v^2q^2}{\delta}\\+i\frac{\eta q^2}{\rho_0}\Omega\end{array}\right)\left(\lambda_Tq^2-i\rho_0c_V\Omega\right)\\-i\left(1-\frac{1}{\delta}\right)\rho_0c_V\Omega v^2q^2\end{array}\right]\\&=E_1E_2^*\left[\begin{array}{l}-\left(i\rho_0c_V\Omega-\lambda_Tq^2\right)\left(\rho_0\frac{\partial\varepsilon}{\partial\rho}\right)_T q^2\\-\frac{2q^2v^2\beta\rho_0}{\delta}\left[nc\alpha_\Sigma-\frac{i}{2}\left(\rho_0\frac{\partial\varepsilon}{\partial\rho}\right)_T\beta T_0\Omega\right]\end{array}\right]\\&=E_1E_2^*\left[\begin{array}{l}-2\beta nc\alpha_\Sigma\rho_0\frac{v^2q^2}{\delta}\\+\left(\rho_0\frac{\partial\varepsilon}{\partial\rho}\right)_T q^2\left[\begin{array}{l}\lambda_Tq^2-i\rho_0c_V\Omega\\+\frac{i}{\delta}v^2\rho_0\beta^2T_0\Omega\end{array}\right]\end{array}\right].\end{aligned}\tag{18}$$

By the use of the expressions $\beta_S(\delta-1)=\frac{\beta^2T_0}{\rho_0c_P}$ and $v^2=\frac{1}{\rho_0\beta_S}$ the other form of the last term in (18) is achieved

$$\begin{aligned}&\frac{i}{\delta}v^2\rho_0\beta^2T_0\Omega=\\&\frac{i}{\delta}v^2\Omega\beta_S(\delta-1)\rho_0^2c_P\\&=i\left(1-\frac{1}{\delta}\right)\rho_0c_P\Omega\end{aligned}\tag{19}$$

From the standpoint of a cubic nonlinear susceptibility tensor, projections of the nonlinear polarization vectors appearing in (11), (12) into the Cartesian coordinates are [37]

$$\begin{aligned}&\left(P^{NL}_{\omega_1,\omega_2}(z,t)\right)_i\\&=\chi^{(3)}_{ijkl}(\omega_1,\omega_2,\Omega)\left(E(z,t)\right)_j\left(E(z,t)\right)_k\left(E(z,t)\right)_l\end{aligned}$$

For our case defined by (7) - (9)):

$$\begin{aligned}&\left(\boldsymbol{P}^{NL}_{\omega_1,\omega_2}\right)_i=\chi^{(3)}_{ixxx}(\boldsymbol{E})^3_x=\chi^{(3)}_{ixxx}(\boldsymbol{E}_P+\boldsymbol{E}_S)^3_x=\\&=\chi^{(3)}_{ixxx}\left[(\boldsymbol{E}_P)^3_x+3(\boldsymbol{E}_P)^2_x(\boldsymbol{E}_S)_x+3(\boldsymbol{E}_P)_x(\boldsymbol{E}_S)^2_x+(\boldsymbol{E}_S)^3_x\right]\end{aligned}$$

For the isotropic branch $\chi^{(3)}$ is a scalar:

$$\begin{aligned}&\left(\boldsymbol{P}^{NL}_{\omega_1,\omega_2}\right)_x=\chi^{(3)}(\boldsymbol{E})^3_x=\chi^{(3)}(\boldsymbol{E}_P+\boldsymbol{E}_S)^3_x=\\&=\chi^{(3)}\left[(\boldsymbol{E}_P)^3_x+3(\boldsymbol{E}_P)^2_x(\boldsymbol{E}_S)_x+3(\boldsymbol{E}_P)_x(\boldsymbol{E}_S)^2_x+(\boldsymbol{E}_S)^3_x\right]\end{aligned}\tag{20}$$

On substitution of $\Delta^{NL}\rho$ from (14) into (10) in accordance with (18), (19), (20) we derive [2]:

$$\chi^{(3)}=\frac{1}{4\pi D}\left(\rho_0\frac{\partial\varepsilon}{\partial\rho}\right)_T\frac{1}{16\pi\rho_0}\times$$
$$\left\{-2\beta nc\alpha_\Sigma\rho_0\frac{v^2q^2}{\delta}+\left(\rho_0\frac{\partial\varepsilon}{\partial\rho}\right)_T q^2\begin{bmatrix}\lambda_T q^2\\ -i\rho_0 c_V\Omega\\ +i\left(1-\frac{1}{\delta}\right)\rho_0 c_P\Omega\end{bmatrix}\right\}\times \quad (21)$$
$$\left\{\begin{bmatrix}-\Omega^2+\frac{v^2q^2}{\delta}\\ +i\frac{\eta q^2}{\rho_0}\Omega\end{bmatrix}\begin{bmatrix}\lambda_T q^2\\ -i\rho_0 c_V\Omega\end{bmatrix}-i\left(1-\frac{1}{\delta}\right)\rho_0 c_V\Omega v^2q^2\right\}^{-1}.$$

In our case $D=3$ [2]. The cubic nonlinear susceptibility (21) exhibits Rayleigh (labeled with R) resonance at $|\Omega|\approx 0$ and Brillouin (labeled with B) resonance at $|\Omega|\approx\Omega_B=qv=(k_1+k_2)v$.

Rayleigh resonances. For $\Omega\approx 0, |\Omega|<<\Omega_B$ (21) incorporates electrocaloric (labeled with R1) and absorptive (labeled with R2) terms:

$$\chi^{(3)R}\approx\chi^{(3)R1}+\chi^{(3)R2}$$

where

$$\chi^{(3)R1}=-\frac{1}{32\pi^2 D}\left(\rho_0\frac{\partial\varepsilon}{\partial\rho}\right)_T^2\beta_S(\delta-1)\begin{bmatrix}\frac{2-\delta}{2(\delta-1)}\\ +\frac{i\Gamma_R}{\Omega+i\Gamma_R}\end{bmatrix} \quad (22)$$

$$\chi^{(3)R2}=\frac{1}{64\pi^2 D}\left(\rho_0\frac{\partial\varepsilon}{\partial\rho}\right)_T\frac{\alpha_\Sigma cn\beta}{\Gamma_R c_P\rho_0}\frac{i\Gamma_R}{\Omega+i\Gamma_R} \quad (23)$$

$$\Gamma_R=\frac{\lambda_T q^2}{\rho_0 c_P}$$

The imaginary parts of (22) and (23) are (as to the origin of β_R^e and β_R^a see (34) below)

$$\begin{aligned}\mathrm{Im}\chi^{(3)R1}&=-\frac{1}{32\pi^2 D}\left(\rho_0\frac{\partial\varepsilon}{\partial\rho}\right)_T^2\beta_S(\delta-1)\frac{\Gamma_R\Omega}{\Omega^2+\Gamma_R^2}\\ &=-\frac{1}{32\pi^2 D}\left(\rho_0\frac{\partial\varepsilon}{\partial\rho}\right)_T^2\beta_S(\delta-1)\frac{\Omega/\Gamma_R}{(\Omega/\Gamma_R)^2+1}\\ &=-\beta_R^e\frac{\Omega/\Gamma_R}{(\Omega/\Gamma_R)^2+1},\end{aligned} \quad (24)$$

$$\begin{aligned}\mathrm{Im}\chi^{(3)R2}&=\frac{1}{64\pi^2 D}\left(\rho_0\frac{\partial\varepsilon}{\partial\rho}\right)_T\frac{\alpha_\Sigma cn\beta}{\Gamma_R c_P\rho_0}\frac{\Gamma_R\Omega}{\Omega^2+\Gamma_R^2}\\ &=\frac{1}{64\pi^2 D}\left(\rho_0\frac{\partial\varepsilon}{\partial\rho}\right)_T\frac{\alpha_\Sigma cn\beta}{\Gamma_R c_P\rho_0}\frac{\Omega/\Gamma_R}{(\Omega/\Gamma_R)^2+1}\\ &=\beta_R^a\frac{\Omega/\Gamma_R}{(\Omega/\Gamma_R)^2+1}.\end{aligned} \quad (25)$$

Brillouin resonances. For $\Omega\approx\pm\Omega_B$ (21) incorporates electrostrictive (or conventional labeled with B1) and absorptive (or thermal labeled with B2) terms:

$$\chi^{(3)B}\approx\chi^{(3)B1}+\chi^{(3)B2}$$

where

$$\chi^{(3)B1}=\frac{1}{64\pi^2 D}\left(\rho_0\frac{\partial\varepsilon}{\partial\rho}\right)_T^2\beta_S(2-\delta)\frac{\rho_0 v}{\eta q}\frac{\Gamma_B/2}{|\Omega|-\Omega_B\pm i\Gamma_B/2} \quad (26)$$

$$\chi^{(3)B2}=\pm\frac{i}{32\pi^2 D}\left(\rho_0\frac{\partial\varepsilon}{\partial\rho}\right)_T\frac{\alpha_\Sigma cn\beta}{\Gamma_B c_P\rho_0}\frac{\Gamma_B/2}{|\Omega|-\Omega_B\pm i\Gamma_B/2} \quad (27)$$

$$\Gamma_B=\frac{\eta q^2}{\rho_0}$$

The bottom signs in (26), (27), (28), and (29) correspond to the stokes ($\omega_1>\omega_2,\ \Omega>0,\ |\Omega|=\Omega$) and the top sings - to the anti-stokes ($\omega_1<\omega_2,\ \Omega<0,\ |\Omega|=-\Omega$) spectral regions, respectively. The imaginary parts of (26) and (27) are (as to the origin of β_B^e and β_B^a see (34) below)

$$\begin{aligned}\mathrm{Im}\chi^{(3)B1}&=\pm\frac{1}{64\pi^2 D}\left(\rho_0\frac{\partial\varepsilon}{\partial\rho}\right)_T^2\beta_S(2-\delta)\frac{\rho_0 v}{\eta q}\frac{\Gamma_B^2/4}{(|\Omega|-\Omega_B)^2+\Gamma_B^2/4}\\ &=\pm\frac{1}{64\pi^2 D}\left(\rho_0\frac{\partial\varepsilon}{\partial\rho}\right)_T^2\beta_S(2-\delta)\frac{\rho_0 v}{\eta q}\frac{1}{\left[2(|\Omega|-\Omega_B)/\Gamma_B\right]^2+1}\\ &=\mp\beta_B^e\frac{1}{\left[2(|\Omega|-\Omega_B)/\Gamma_B\right]^2+1}.\end{aligned} \quad (28)$$

$$\begin{aligned}\mathrm{Im}\chi^{(3)B2}&=\pm\frac{1}{32\pi^2 D}\left(\rho_0\frac{\partial\varepsilon}{\partial\rho}\right)_T\frac{\alpha_\Sigma cn\beta}{\Gamma_B c_P\rho_0}\frac{(|\Omega|-\Omega_B)\Gamma_B/2}{(|\Omega|-\Omega_B)^2+\Gamma_B^2/4}\\ &=\pm\frac{1}{32\pi^2 D}\left(\rho_0\frac{\partial\varepsilon}{\partial\rho}\right)_T\frac{\alpha_\Sigma cn\beta}{\Gamma_B c_P\rho_0}\frac{2(|\Omega|-\Omega_B)/\Gamma_B}{\left[2(|\Omega|-\Omega_B)/\Gamma_B\right]^2+1}\\ &=\mp\beta_B^a\frac{2(|\Omega|-\Omega_B)/\Gamma_B}{\left[2(|\Omega|-\Omega_B)/\Gamma_B\right]^2+1}.\end{aligned} \quad (29)$$

A couple of equal in magnitude to

$$\mathrm{Im}\chi^{(3)\mathrm{B1}}_{\mathrm{MAX}} = \frac{1}{64\pi^2 \mathrm{D}}\left(\rho_0 \frac{\partial \varepsilon}{\partial \rho}\right)^2_{\mathrm{T}} \beta_{\mathrm{S}}(2-\delta)\frac{\rho_0 \mathrm{v}}{\eta \mathrm{q}} = \frac{\beta_{\mathrm{S}}(2-\delta)\Omega_{\mathrm{B}}}{64\pi^2 \mathrm{D}\Gamma_{\mathrm{B}}}\left(\rho_0 \frac{\partial \varepsilon}{\partial \rho}\right)^2_{\mathrm{T}} \quad (30)$$

peaks of the electrostrictive (conventional) Brillouin term defined by (28) demonstrate positive $G \propto -Im\chi^{(3)}$ for $\Omega \approx \Omega_{\mathrm{B}}$, and negative $G \propto -Im\chi^{(3)}$ for $\Omega \approx -\Omega_{\mathrm{B}}$ (Fig. 1a).

Four equal in magnitude to

$$\mathrm{Im}\,\chi^{(3)\mathrm{B2}}_{\mathrm{MAX}} = \frac{1}{32\pi^2 \mathrm{D}}\left(\rho_0 \frac{\partial \varepsilon}{\partial \rho}\right)_{\mathrm{T}} \frac{\alpha_\Sigma \mathrm{c\,n}\beta}{\Gamma_{\mathrm{B}} c_{\mathrm{P}} \rho_0} \frac{\Gamma^2_{\mathrm{B}}/4}{\Gamma^2_{\mathrm{B}}/4 + \Gamma^2_{\mathrm{B}}/4} = \frac{\alpha_\Sigma \mathrm{c\,n}\beta}{64\pi^2 \mathrm{D}\,\Gamma_{\mathrm{B}} c_{\mathrm{P}} \rho_0}\left(\rho_0 \frac{\partial \varepsilon}{\partial \rho}\right)_{\mathrm{T}} \quad (31)$$

peaks of the absorptive (thermal) Brillouin term defined by (29) demonstrate positive and negative $G \propto -Im\chi^{(3)}$ both for $\Omega \approx \Omega_{\mathrm{B}}$ and for $\Omega \approx -\Omega_{\mathrm{B}}$ (Fig. 1b). The ratio of (31) and (30) provides the relative contribution of the absorptive (thermal) and electrostrictive (conventional) mechanisms into SBS gain (see Section 7):

$$\frac{\mathrm{Im}\chi^{(3)\mathrm{B2}}_{\mathrm{MAX}}}{\mathrm{Im}\chi^{(3)\mathrm{B1}}_{\mathrm{MAX}}} = \left(\frac{\alpha_\Sigma \mathrm{c\,n}\beta}{64\pi^2 \mathrm{D}\Gamma_{\mathrm{B}} c_{\mathrm{P}} \rho_0}\left(\rho_0 \frac{\partial \varepsilon}{\partial \rho}\right)_{\mathrm{T}}\right)\left(\frac{64\pi^2 \mathrm{D}\Gamma_{\mathrm{B}}}{\beta_{\mathrm{S}}(2-\delta)\Omega_{\mathrm{B}}}\left(\rho_0 \frac{\partial \varepsilon}{\partial \rho}\right)^{-2}_{\mathrm{T}}\right) = \frac{\alpha_\Sigma \mathrm{c\,n}\beta}{c_{\mathrm{P}} \rho_0 \beta_{\mathrm{S}}(2-\delta)\Omega_{\mathrm{B}}}\left(\rho_0 \frac{\partial \varepsilon}{\partial \rho}\right)^{-1}_{\mathrm{T}} = \frac{(\delta-1)}{(2-\delta)}\frac{\alpha_\Sigma \mathrm{c\,n}}{\beta \mathrm{T}_0 \Omega_{\mathrm{B}}}\left(\rho_0 \frac{\partial \varepsilon}{\partial \rho}\right)^{-1}_{\mathrm{T}} = \frac{(\delta-1)}{(2-\delta)}\frac{\alpha_\Sigma \lambda_1}{4\pi\beta \mathrm{T}_0}\frac{\mathrm{c/v}}{\sin(\theta/2)}\left(\rho_0 \frac{\partial \varepsilon}{\partial \rho}\right)^{-1}_{\mathrm{T}}, \quad (32)$$

where

$$\frac{\beta}{\beta_S} = \frac{\rho_0 c_P(\delta-1)}{\beta T_0}, \quad \lambda_1 = \frac{2\pi c}{\omega_1}, \quad k_1 = \frac{2\pi n}{\lambda_1},$$

$$\Omega_B = qv = 2k_1 v \sin(\theta/2) = \frac{4\pi v n}{\lambda_1}\sin(\theta/2)$$

λ_1 is the pump wavelength and θ is the angle of scattering.

On substitution of the resulting expressions for $\boldsymbol{P}^{NL}$ into (11), (12) we derive a system [17]:

$$\left(\frac{\partial}{\partial z} + \alpha_\Sigma\right)\left|E_1(z)\right|^2 = -G\left|E_1(z)\right|^2\left|E_2(z)\right|^2,$$

$$\left(\frac{\partial}{\partial z} - \alpha_\Sigma\right)\left|E_2(z)\right|^2 = -G\left|E_1(z)\right|^2\left|E_2(z)\right|^2. \quad (33)$$

Following (33), when the pump intensity $I_P(z) \propto |E_1(z)|^2$ is treated as constant over the length L of nonlinear interaction, the scattered wave intensity $I_S(z) \propto |E_2(z)|^2$ exponentially increases along z with a gain coefficient

$$g = G\left|E_1\right|^2 - \alpha_\Sigma,$$

where $G \propto -Im\chi^{(3)}$ is a gain parameter. The general formula for G is [17] (See (24), (25), (28), and (29))

$$\mathrm{G}(\Omega) = \pm\beta^{\mathrm{e}}_{\mathrm{B}}\frac{1}{1+(2\Delta\Omega/\Gamma_{\mathrm{B}})^2} \pm\beta^{\mathrm{a}}_{\mathrm{B}}\frac{2\Delta\Omega/\Gamma_{\mathrm{B}}}{1+(2\Delta\Omega/\Gamma_{\mathrm{B}})^2} + (\beta^{\mathrm{e}}_{\mathrm{R}} - \beta^{\mathrm{a}}_{\mathrm{R}})\frac{\Omega/\Gamma_{\mathrm{R}}}{1+(\Omega/\Gamma_{\mathrm{R}})^2}, \quad (34)$$

where

$$\Omega = \omega_1 - \omega_2, \ \Delta\Omega = |\Omega| - \Omega_B, \ \Omega_B = (k_1 + k_2)v,$$

$$\Gamma_B = \frac{\eta(k_1+k_2)^2}{\rho_0}, \ \Gamma_R = \frac{\lambda_T(k_1+k_2)^2}{\rho_0 C_P}. \quad (35)$$

In the first two expressions of (34) signs "+" and "-" correspond to the stokes ($\omega_1 > \omega_2, \Omega > 0$) and anti-stokes ($\omega_1 < \omega_2, \Omega < 0$) spectral regions, respectively.

5. SBS and ST Spectral Components for Linear Absorption

Fig. 1 shows the spectral profiles of $G(\Omega)$ for the SBS and STS mechanisms. For linear absorption such curves can be found in [2, 18]. A couple of the SBS curves in the vicinity of the stokes resonance can be found in [4, 17]. Excitation of an anti-stokes SBS component was not considered there.

The term proportional to β^e_B in (34) represents the conventional SBS. The spectral profile (Fig. 1a) possesses positive stokes and negative anti-stokes values. The widths (FWHM) of resonance peaks are approximately equal to Γ_B.

The term proportional to $\beta^a_B \propto \alpha_\Sigma = \alpha$ (see (29)) represents the linear thermal SBS. The spectral profile (Fig. 1b) possesses positive and negative values in both stokes and anti-stokes regions. The widths (FWHM) of resonance

peaks are approximately equal to $\Gamma_B / 2$.

The term proportional to $\beta_R^a \propto \alpha_\Sigma = \alpha$ (see (25)) represents the STS due to linear absorption (the linear STS-2). The spectral profile (Fig. 1b) possesses positive anti-stokes and negative stokes values. The widths (FWHM) of resonance peaks are approximately equal to Γ_R.

The term proportional to β_R^e represents the STS due to an electrocaloric effect (the STS-1). The spectral profile (Fig. 1a) is mirror symmetric to that of the linear STS-2.

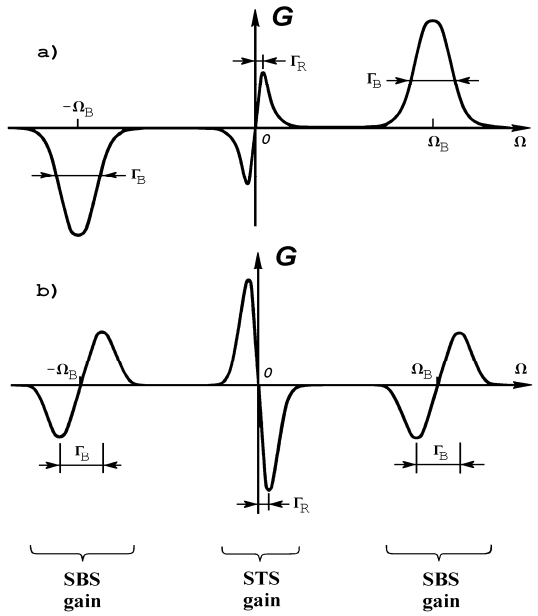

Figure 1. *The gain parameter $G(\Omega)$ defined by (34) for the SBS and STS mechanisms: (a) conventional SBS and STS-1; (b) thermal SBS and STS-2.*

6. SBS and STS Spectral Components for Two-Photon Absorption

Single-photon and two-photon transitions provide complementary spectroscopic data [17]. In analysis [5] linear (single-photon) absorption switches to two-photon one by replacing α with γI_P. In particular, $\beta_R^a, \beta_B^a \propto \gamma I_P$.

Being essentially different [5], the linear STS-2 and two-photon STS-2 are characterized by the common gain curve (Fig. 1b). The shifts and widths of its resonance peaks are approximately equal to Γ_R, which is close to the spectral resolution of the typical experimental setup [5]. In this respect, the linear and two-photon STS-2 spectral components are experimentally indistinguishable not only from one another, but also from the STS-1 one, characterized by the mirror symmetric gain curve (Fig. 1a).

SBS contains the experimentally distinguishable [17] conventional and thermal components ($\Omega_B >> \Gamma_B >> \Gamma_R \approx$ spectral resolution). In the stokes region the conventional SBS must be shifted by the thermal SBS. For linear absorption such a shift depends on α. For two-photon absorption such a shift depends on γI_P (see Section 7). In the anti-stokes region the positive two-photon thermal values, being proportional to $\beta_B^a \propto I_P$, are added to the negative conventional values, being proportional to $\beta_B^e = \text{const}$, and the positive overall SBS gain can be achieved when I_P is sufficiently high.

7. Overall Stokes SBS Gain

Denoting the stokes SBS part of (34) by β_B and dividing it by β_B^e, we obtain

$$\left(\beta_B / \beta_B^e\right) = \frac{1}{1+\left(2\Delta\Omega / \Gamma_B\right)^2} + \left(\beta_B^a / \beta_B^e\right)\frac{2\Delta\Omega / \Gamma_B}{1+\left(2\Delta\Omega / \Gamma_B\right)^2} . \quad (36)$$

Setting

$$\left(\beta_B / \beta_B^e\right) \equiv Z, \quad \left(\beta_B^a / \beta_B^e\right) \equiv Y, \quad \left(2\Delta\Omega / \Gamma_B\right) \equiv X ,$$

we rewrite (36) as

$$Z(X,Y) = \frac{1}{1+X^2} + Y\frac{X}{1+X^2} . \quad (37)$$

The parameters β_B^a, β_B^e, and Γ_B are independent of $\Delta\Omega$. A variable X in (37) describes the frequency shift $\Delta\Omega$. When $X = 1$, the shift is $\Delta\Omega = \Gamma_B / 2$. A variable $Y \geq 0$ expresses a relative contribution of the thermal and conventional SBS. $Y < 1$ is the realistic case of strong conventional and weak thermal mechanisms; and $Y > 1$ is the unrealistic case because of the self-action and phase mismatch due to heating [5]. For linear absorption [2, 4] (see (32))

$$Y = \frac{\beta_B^a}{\beta_B^e} = \frac{\delta - 1}{2 - \delta}\frac{\alpha\lambda_1}{4\pi\beta T_0}\frac{c / v}{\sin(\theta/2)\rho_0\left(\partial\varepsilon/\partial\rho\right)_T} , \quad (38)$$

where $\theta = \pi$ for the backscattering. Thus,

$$Y = (\text{const}) \times \alpha . \quad (39)$$

For two-photon absorption α is substituted by γI_P in (38), and

$$Y = (\text{const}) \times (\gamma I_P) . \quad (40)$$

According to (39) and (40), when the material properties are held constant ($\alpha, \gamma = \text{const}$), a change in I_P can cause a change in Y for the two-photon thermal SBS, only.

A function $Z(X,Y)$ can be treated as a dependence $\text{const}\times\beta_B(X)$ at different values of Y. Fig. 2 shows a three-dimensional plot of $Z=Z(X,Y)$ for Y varying from 0 to 1.5. The intersection of $Z(X,Y)$ with the plane $Y=0$ is the even function of X corresponding to the conventional SBS. The contour plot in Fig. 3 demonstrates the shift more clearly.

The experimentally observed stimulated scattering spectral components are 5-times narrower [15] than the gain curves in Figs. 2 and 3. Hence, in an experiment the extra shift must be more pronounced.

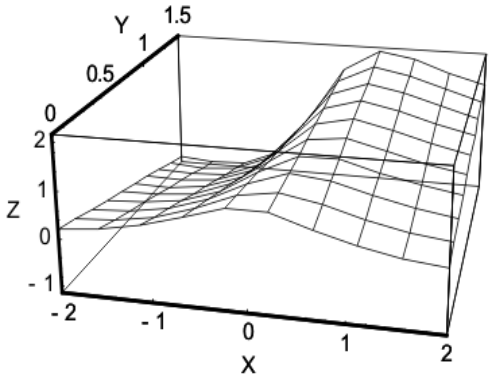

Figure 2. *A three-dimensional plot of the overall stokes SBS gain parameter for the conventional and thermal mechanisms.*

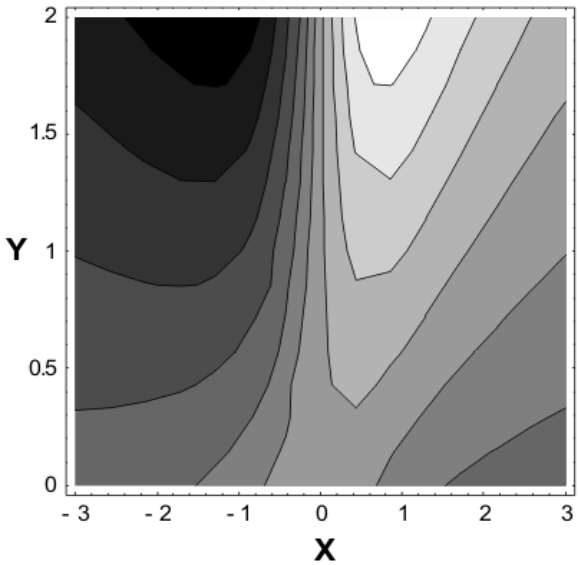

Figure 3. *The contour plot corresponding to Fig. 2. The gray-scale legend is evident from Fig. 2.*

8. Numerical Estimates for Spectral Shift

According to the relaxation theory developed by Mandelstam and Leontovich, attenuation of a hypersonic wave in a liquid is dominated by shear viscosity [21, 34, 35, 38]. Therefore,

$$\eta\approx\frac{2\eta_1}{3},\quad k_1+k_2\approx 2k_1=\frac{4\pi n}{\lambda_1},$$

where η_1 is a shear viscosity coefficient. From (35) we obtain

$$\Gamma_B=\frac{2\eta_1}{3\rho_0}\left(\frac{4\pi n}{\lambda_1}\right)^2=\frac{32\,\pi^2 n^2\eta_1}{3\rho_0\lambda_1^2}. \qquad (41)$$

Following [5], we perform estimates for liquid hexane (C6H14), $\lambda_1=308\ nm$, and the material parameters [1, 21, 38, 39]:

$$\lambda_1\approx 3\times10^{-5}\ \text{cm},\ \theta=\pi,\ \rho_0\approx 0.66\,\frac{\text{g}}{\text{cm}^3},\ n\approx 1.4,$$

$$\eta_1\approx 3.2\times10^{-3}\,\text{P}\approx 3.2\times10^{-3}\,\frac{\text{g}}{\text{cm s}},$$

$$\beta\approx 1.4\times10^{-3}\,\text{K}^{-1},\ T_0\approx 300\ \text{K},$$

$$v\approx 10^5\,\frac{\text{cm}}{\text{s}},\ c\approx 3\times10^{10}\,\frac{\text{cm}}{\text{s}},\ \rho_0\left(\frac{\partial\varepsilon}{\partial\rho}\right)_T\approx 1,\ \delta=\frac{C_P}{C_V}\approx 1.3.$$

Then (41) yields

$$\Gamma_B\approx 1.1\times10^9\,Hz\approx 0.03\ cm^{-1}.$$

Equation (38) gives

$$Y=\frac{\beta_B^a}{\beta_B^e}\approx 0.73\times\alpha, \qquad (42)$$

where α is measured in cm^{-1}. $Y=1$ corresponds to $\alpha=1.37\ cm^{-1}$.

For two-photon absorption α is substituted by γI_P in (42), and

$$Y=0.73\times(\gamma I_P). \qquad (43)$$

Table 1 from [5] lists the two-photon contribution γI_P obtained for the three experimental values of I_P. The maximum value is $(\gamma I_P^{max})\approx 1\ cm^{-1}$ and

$$Y^{max}=0.73\times(\gamma I_P^{max})\approx 0.73.$$

Due to losses and saturation the stimulated scattering is generated near the top of the curve in Fig. 2. Hence, from Fig. 3 $Y\approx 0.73$ corresponds to $X\approx 0.5$, and the frequency shift is

$$\Delta\Omega\approx\frac{\Gamma_B}{4}\approx 0.007\,cm^{-1}.$$

It should be noted that the SBS component was suppressed at I_P^{max} because of the phase mismatch associated

with the two-photon heating [5]. For $I_P \approx 10^9 W/cm^2$ we have $(\gamma I_P) \approx 0.1\, cm^{-1}$ (see Table 1) and $Y \approx 0.07$ (see (43)). The appropriate shift (see Fig. 3) is too small, to be detected under the experimental conditions of [5]. This is not surprising because the analysis presented in [5] was focused on other issues.

Table 1. *Two-photon contribution γI_P to the total absorption coefficient at λ_1=308nm in hexane for the three values of the pump intensity I_P*

I_P, W/cm^2	γI_P, cm^{-1}
$\geq 10^{10}$	≥ 1.0
10^9	≈ 0.1
2.5×10^8	≈ 0.025

9. Conclusions

The basic equations describing SBS and STS are used to determine the spectral profiles of the gain. The linear (single-photon) and two-photon absorptions are compared.

In the stokes region the conventional SBS is shifted by the thermal SBS. In contrast to linear absorption, for two-photon one this shift depends on the pump intensity I_P. In the anti-stokes region the positive two-photon thermal gain being proportional to I_P is added to the negative conventional gain, and the positive overall SBS gain can be achieved when I_P is sufficiently high.

Estimates made for liquid hexane and the pump wavelength $308\,nm$ show that the typical extra shift of the stokes SBS component is $0.007 cm^{-1}$. The spectral resolution of a Fabry-Perot etalon is limited by several MHz (or $10^{-3}\ cm^{-1}$). To reach the higher spectral resolution the methods of heterodyning and intensity fluctuations correlation should be used.

For a Fabry-Perot etalon based spectrum analyzer the linear STS-2 and two-photon STS-2 components are experimentally indistinguishable not only from one another, but also from the STS-1 component.

References

[1] S.Kielich, Molecular Nonlinear Optics. Warsaw: PWN, 1977 [Moscow: Nauka, 1981].

[2] S.A.Akhmanov and N.I.Koroteev, Methods of Nonlinear Optics in Spectroscopy of Light Scattering. Moscow: Nauka, 1981 [in Russian].

[3] D.H.Rank, C.W.Cho, N.D.Foltz, and T.A.Wiggins, "Stimulated thermal Rayleigh scattering", Phys. Rev. Lett., vol. 19, pp. 828-830, 1967.

[4] V.S.Starunov and I.L.Fabelinskii, "Stimulated Mandel'shtam-Brillouin scattering and stimulated entropy (temperature) scattering of light", Sov. Phys. Usp., vol. 12, pp. 463-489, 1970 [Usp. Fiz. Nauk, vol. 98, pp. 441-491, 1969].

[5] V.B.Karpov and V.V.Korobkin, "Stimulated thermal scattering induced by two-photon absorption and experimental observation of genuine stimulated Brillouin scattering in the near-ultraviolet region", Phys. Rev. A, vol. 77, p. 063812, 2008.

[6] B.J.Feldman, R.A.Fisher, A.Robert, and S.L.Shapiro, "Ultraviolet phase conjugation", Optics Letters, vol. 6, No. 2, pp. 84-86, 1981.

[7] R.G.Caro and M.C.Gower, "Phase conjugation of KrF laser radiation", Optics Letters, vol. 6, pp. 557-559, 1981.

[8] M.C.Gower and R.G.Caro,"KrF laser with a phase-conjugate Brillouin mirror", Optics Letters, vol. 7, No. 4, pp. 162-164, 1982.

[9] M.C.Gower, "KrF laser amplifier with phase-conjugate Brillouin retroreflectors", Optics Letters, vol. 7, No. 9, pp. 423-425, 1982.

[10] E.Armandillo and D.Proch, "Highly efficient, high-quality phase-conjugate reflection at 308nm using stimulated Brillouin scattering", Optics Letters, vol. 8, No. 10, pp. 523-525, 1983.

[11] M.C.Gower, "Phase conjugation at 193nm", Optics Letters, vol. 8, No. 2, pp. 70-72, 1983.

[12] G.M.Davis and M.C.Gower, "Stimulated Brillouin scattering of a KrF laser", IEEE J. Quant. Electron., vol. 27, No. 3, pp. 496-501, 1991.

[13] S.S.Alimpiev, V.S.Bukreev, S.K.Vartapetov, I.A.Veselovskii, V.S.Nersisian, A.Z.Obidin, and A.M.Prokhorov, "Line narrowing and wavefront reversal of radiation of an XeCl laser ", Sov. Phys.-Lebedev Inst. Reports, No. 12, pp. 12-15, 1989 [Kratk. Soobshch. Fiz., No. 12, pp. 11-13, 1989].

[14] S.S.Alimpiev, V.S.Bukreev, S.K.Vartapetov, I.A.Veselovskii, B.I.Kusakin, S.V.Lihanckii, and A.Z.Obidin, "Line narrowing and wavefront reversal of radiation of an KrF laser", Quant. Electron., vol. 21, pp.80-81, 1991 [Kvant. Elektron. (Moscow), vol. 18, pp. 89-90, 1991].

[15] B.Ya.Zeldovich, N.F.Pilipetsky, and V.V.Shkunov, Principles of Phase Conjugation. Berlin: Springer, 1985 [Moscow: Nauka, 1985].

[16] V.G.Dmitriev, Nonlinear Optics and Phase Conjugation. Moscow: Fizmatlit, 2003 [in Russian].

[17] Y.R.Shen, The Principles of Nonlinear Optics. New York: Wiley-Interscience, 1984 [Moscow: Nauka, 1989].

[18] B.Ya.Zel'dovich and I.I.Sobel'man,, "Stimulated light scattering induced by absorption", Sov. Phys. Usp., vol. 13, pp. 307-317, 1970 [Usp. Fiz. Nauk, vol. 101, pp. 3-20, 1970].

[19] N.M.Kroll, "Excitation of hypersonic vibrations by means of photoelastic coupling of high-intensity light waves to elastic waves ", J. Appl. Phys., vol. 36, pp. 34-44, 1965.

[20] C.L.Tang, "Saturation and spectral characteristics of the stokes emission in the stimulated Brillouin process", J. Appl. Phys., vol. 37, pp. 2945-2956, 1966.

[21] I.L.Fabelinskii, Molecular Scattering of Light. New York:

Plenum, 1968 [Moscow: Nauka, 1965].

[22] N.Bloembergen, Nonlinear Optics. New York: W.A.Benjamin Inc., 1965 [Moscow: Mir, 1966].

[23] R.M.Herman and M.A.Gray, "Theoretical prediction of the stimulated thermal Rayleigh scattering in liquids", Phys. Rev. Lett., vol. 19, pp. 824-828, 1967.

[24] [M.A.Gray and R.M.Herman, "Nonlinear thermal Rayleigh scattering in gases", Phys. Rev., vol. 181, pp. 374-379, 1969.

[25] R.N.Enns and I.P.Batra, "Stimulated thermal scattering in the second-sound regime", Phys. Rev., vol. 180, pp. 227-232, 1969.

[26] J.M.Vaughan, "Correlation analysis and interoferometry in laser spectroscopy of scattering", in Photon Correlation and Light Beating Spectroscopy, H.Z.Cummins and E.R.Pike, Eds. New York: Plenum, 1974, pp. 432-458 [Moscow: Mir, 1978].

[27] E.R.Pike, "Theory of light scattering", in Photon Correlation and Light Beating Spectroscopy, H.Z.Cummins and E.R.Pike, Eds. New York: Plenum, 1974, pp. 17-45 [Moscow: Mir, 1978].

[28] L.D.Landau and E.M.Lifshitz, Mechanics, Course of Theoretical Physics, vol. 1. Oxford: Pergamon, 1976 [Moscow: Nauka, 1988].

[29] L.G.Loitsianskii, Mechanics of Liquids and Gases. Oxford: Pergamon, 1966 [Moscow: Drofa, 2003].

[30] L.D.Landau and E.M.Lifshitz, Theory of Elasticity, Course of Theoretical Physics, vol. 7. Oxford: Pergamon, 1986 [Moscow: Nauka, 1987].

[31] J.Lamb, "Thermal relaxation in liquids", in Physical Acoustics Principles and Methods, vol. II Part A, Properties of Gases, Liquids and Solutions, W.P.Mason, Ed. New York: Academic, 1965, pp. 222-297 [Moscow: Mir, 1968].

[32] A.Bambini, R.Vallauri, and M.Zoppi, "Nonlinear spectroscopy of Rayleigh and Mandel'stan-Brillouin scattering in liquids", in Nonlinear Spectroscopy, N.Bloembergen, Ed. Amsterdam: North-Holland Publ. Comp., 1977, pp. 569-582 [Moscow: Mir, 1979].

[33] V.E.Gusev and A.A.Karabutov, Laser Optical Acoustics. Moscow: Nauka, 1991 [in Russian].

[34] I.G.Mikhailov, V.A.Solov'ev, and Yu.P.Syrnikov, Fundamentals of Molecular Acoustics. Moscow: Nauka, 1964 [in Russian].

[35] L.D.Landau and E.M.Lifshitz, Hydrodynamics, Course of Theoretical Physics, vol. 6. Oxford: Pergamon, 1984 [Moscow: Nauka, 1986].

[36] L.D.Landau and E.M.Lifshitz, Electrodynamics of Continuous Media, Course of Theoretical Physics, vol. 8. Oxford: Pergamon, 1984 [Moscow: Nauka, 1982].

[37] S.A.Akhmanov and R.V.Khokhlov, Problems of Nonlinear Optics 1962-1963. Moscow: VINITI, 1964 [in Russian].

[38] V.F.Nozdrev, The Use of Ultrasonics in Molecular Physics. Oxford: Pergamon, 1965 [Moscow: Fizmatlit, 1958].

[39] M.I.Shakhparonov, Methods for Studying Heat Motion of Molecules and Structure of Liquids. Moscow: Moscow State University Press, 1963 [in Russian].